GPS Solutions (2023) 27:70
https://doi.org/10.1007/s10291-023-01405-9

RESEARCH

Correcting antenna phase center effects to reconcile the code/phase bias products from the third IGS reprocessing campaign

Jihang Lin[1] · Jianghui Geng[1,2] · Zhe Yan[1] · Salim Masoumi[3] · Qiyuan Zhang[1]

Received: 8 August 2022 / Accepted: 18 January 2023 / Published online: 15 February 2023

Abstract

The International GNSS Service aims to provide combined satellite clock and code/phase bias products in the recent third reprocessing campaign (Repro3) to enable more robust ambiguity resolution in precise point positioning (PPP-AR). However, the interoperability of the code/phase bias products from different analysis centers (ACs) was seriously corrupted by their inconsistent corrections of GPS Block III and Galileo satellite antenna phase center (APC) effects. To achieve a sufficient and rapid reconciliation among the Repro3 bias products, we correct efficiently only for the antenna phase center offsets in the radial direction (i.e., z-PCOs), rather than ask each AC to reprocess their 25 years of products by strictly correcting for APC effects repeatedly. A clock/bias combination for 2020 demonstrates that our approximate APC correction significantly reduces the inconsistency among ACs' satellite clock/bias products. The mean residuals from the combination of differential code biases and wide-lane phase biases are within 0.1 ns and 0.03 cycles, respectively. A 30-day PPP-AR test using GPS and Galileo data from 90 stations shows that our combination clock/bias products can still guarantee a wide-lane ambiguity fixing rate that differs by less than 0.5% from that resulting from APC strictly corrected combination products.

Keywords Precise point positioning · Phase center offset · Clock/bias combination · Code/phase bias · GNSS reprocessing campaign

Abbreviations

AC	(Analysis center)
ANTEX	(Antenna Exchange)
APC	(Antenna phase center)
BDS	(Beidou navigation satellite system)
CNES	(Centre National d'Études Spatiales)
CODE	(Center for Orbit Determination in Europe)
DCB	(Differential code bias)
FOC	(Full Operational Capability)
GF	(Geometry-free)
GNSS	(Global navigation satellite system)
GPS	(Global positioning system)
HMW	(Hatch–Melbourne–Wübbena)
IF	(Ionospheric-free)
IGS	(The International GNSS Service)
IOV	(In-Orbit Validation)
LOS	(Line-of-sight)
NRCan	(Natural Resources Canada)
OSB	(Observable-specific bias)
PCO	(Phase center offset)
PCV	(Phase center variation)
PPP-AR	(Precise point positioning with ambiguity resolution)
Repro3	(The third reprocessing campaign)
RMS	(Root mean square)
STD	(Standard deviation)
TUG	(Technical University of Graz)
UPD	(Uncalibrated phase delay)
WHU	(Wuhan University)
WL	(Wide-lane)

✉ Jianghui Geng
jgeng@whu.edu.cn

[1] GNSS Research Center, Wuhan University, Wuhan, China

[2] Hubei Luojia Laboratory, Wuhan, China

[3] Geoscience Australia, Canberra, Australia

Introduction

The pre-calibration of code/phase biases is a prerequisite for achieving ambiguity resolution in precise point positioning (PPP-AR; Ge et al. 2008; Geng et al. 2009). In recent years, several International GNSS Service (IGS; Johnston et al. 2017) Analysis Centers (ACs) have begun to release

routine code/phase bias products for PPP-AR (Laurichesse 2011; Geng et al. 2019b; Schaer et al. 2021). In the third reprocessing campaign (Repro3), the IGS PPP-AR Working Group (https://igs.org/wg/ppp-ar/) attempted to combine AC specific clock/bias products to facilitate and improve PPP-AR (Villiger and Dach 2021). Banville et al. (2020) combined GPS clock/bias products from six ACs over a week in 2018 and verified their millimeter-level consistency or high interoperability. However, recent combination practice shows that the consistency of these ACs' bias products for GPS Block III and Galileo satellites is corrupted due to different correction strategies for their frequency-specific antenna phase center (APC) effects (see IGSMAIL-8113). When applying these bias products in PPP-AR, processing options must be switched depending on whether they have APC corrections applied or not (Geng et al. 2021b). These differences imply that the interoperability of these bias products is compromised.

Geometry-free (GF) observations are often used to compute code biases (Schaer 1999) and wide-lane phase biases (Ge et al. 2008). These observations eliminate all common errors on both frequencies, including satellite APC effects for the early blocks of GPS satellites. Although these APCs are inherently frequency specific, the GNSS community has long used the re-estimated ionospheric-free (IF) APCs, which are presumed identical on the L1/L2 frequencies for these GPS satellites (Schmid and Rothacher 2003; Schmid et al. 2007) due to the controversy over the accuracy and completeness of the manufacturers' APC calibrations (Dilssner 2010; Dilssner et al. 2016). However, for the Galileo and GPS Block III satellites, frequency-specific APC calibrations (European GNSS Agency 2017; Steigenberger et al. 2020) were adopted in the IGS Antenna Exchange (ANTEX; Rothacher and Schmid 2010) files in 2017 and 2019, respectively. As a result, geometry-free linear combinations cannot cancel the frequency-specific APC effects, and both code biases and wide-lane phase biases will be affected.

IGS ACs are now using different processing strategies to estimate their clock/bias products for IGS Repro3. Significant offsets among these products were observed in the clock/bias combination due to different strategies in correcting for APC effects. For example, when estimating the wide-lane phase biases, the Center for Orbit Determination in Europe (CODE; Dach et al. 2021; Schaer et al. 2021) and the Centre National d'Études Spatiales (CNES; Loyer et al. 2012; Katsigianni et al. 2019) use Hatch–Melbourne–Wübbena (HMW; Hatch 1982; Melbourne 1985; Wübbena 1985) observations without APC corrections; Natural Resources Canada (NRCan) uses the same HMW observations (Collins et al. 2010) but with APC corrections applied; the Technical University of Graz (TUG) is the only AC that uses the raw observations approach (Strasser et al. 2019; Strasser 2022), where APC corrections are bound to be applied. Similar offsets were also found between the differential code biases (DCBs) from CODE's ionosphere analysis (Schaer 1999) and TUG.

At the IGS 2022 Virtual Workshop, ACs reached consensus on correcting antenna phase center effects in the generation of clock/bias products (Geng 2022). As a compromise to reconcile the existing AC specific clock/bias products for IGS Repro3, we propose an approximate but efficient method to correct only for the satellite antenna phase center offsets (PCOs) in the radial direction (i.e., z-PCOs) and ignore the minor effects caused by other components of the PCOs and their variations (PCVs), rather than ask each AC to reprocess their 25 years of products repeatedly. This method does not require re-estimation of any Repro3 products and thus saves a considerable amount of computation resources.

In this contribution, we first demonstrate how the uncorrected frequency-specific APC effects in geometry-free observations affect the code/phase biases and the feasibility of approximating the true APC effects with the z-PCOs only. Specific correction equations for different forms of code/phase biases are then derived. The effectiveness of our approximate APC corrections is verified by a one-year period combination test, where the consistency among ACs' bias products is significantly improved. Finally, the APC approximately corrected and APC strictly corrected combined biases are compared in PPP-AR processing and show equivalent results.

APC effects on code/phase biases

GNSS signals are transmitted or received at the phase center of the antenna, which differs from the reference point of the satellite or receiver antenna used to calculate distances in the geometric model. To present the APC effects on different code/phase biases, we start with the raw phase (L_i) and code (P_i) observation equations on frequency f_i as follows

$$L_i = \rho + s_i + b_i + \gamma_i^2 I + \lambda_i N_i \tag{1}$$

$$P_i = \rho + s_i + d_i - \gamma_i^2 I \tag{2}$$

The first thing to notice is that symbol s_i is used to denote the frequency-specific APC effect on the raw observations, which is presumed identical for both phase and code observations on the same frequency and ignores the group delay variations (Wanninger et al. 2017). The nominal geometric distance ρ represents all frequency-independent effects, including clock offset and tropospheric delay. The phase bias b_i and code bias d_i are defined in an observation-specific representation according to the Bias-SINEX format (Schaer 2016). I is the ionospheric delay on the first frequency f_1 and $\gamma_i^2 = f_1^2/f_i^2$ is the squared frequency ratio. λ_i is the

wavelength and N_i is the integer ambiguity of phase observations. The observation noise and other effects are ignored. For simplicity, similar effects from satellites and receivers are given here in an integrated form, although the difference between APC effects from satellite and receiver antennas will be investigated later.

Since the code/phase biases are highly correlated with other effects such as clock errors and atmospheric delays (Håkansson et al. 2017), it is essential to separate them in the estimation. When raw observations are directly utilized to estimate code/phase biases, accurate a priori models are needed to correct for various modelable terms including APC effects, while parameters such as clock errors and atmospheric delays are estimated in advance and fixed (Strasser et al. 2019). Similar strategies are also applied to other geometry-preserving approaches to estimate code/phase biases, for example, estimating the narrow-lane phase biases with the ionospheric-free observations (Geng et al. 2019b). However, APC corrections are normally neglected and not applied on the geometry-free observations (Laurichesse et al. 2009; Loyer et al. 2012), leaving them subject to the frequency-specific APC effects. The geometry-free observations commonly used for code/phase bias estimation are the geometry-free linear combination and the Hatch–Melbourne–Wübbena linear combination.

Geometry-free linear combination

The geometry-free (GF) linear combination is

$$\begin{aligned} P_{\mathrm{GF}} =& P_1 - P_2 \\ =& s_{\mathrm{GF}} + d_{\mathrm{GF}} + (1-\gamma_2^2)I \end{aligned} \tag{3}$$

where

$$s_{\mathrm{GF}} = s_1 - s_2 \tag{4}$$

$$d_{\mathrm{GF}} = d_1 - d_2 \tag{5}$$

d_{GF} is known as the inter-frequency DCB. It is often provided by analysis centers as a by-product of ionosphere analysis (Schaer 1999). In the case of estimating satellite DCBs with ionosphere analysis, s_{GF} can mostly be absorbed into d_{GF} since the satellite APC effects on all ground stations are almost identical (Geng et al. 2021a).

Hatch–Melbourne–Wübbena linear combination

The Hatch–Melbourne–Wübbena (HMW) linear combination is

$$\begin{aligned} L_{\mathrm{HMW}} =& \frac{1}{\gamma_2-1}\left(\gamma_2 L_1 - L_2\right) - \frac{1}{\gamma_2+1}\left(\gamma_2 P_1 + P_2\right) \\ =& s_{\mathrm{HMW}} + b_{\mathrm{HMW}} + \lambda_{\mathrm{WL}} N_{\mathrm{WL}} \end{aligned} \tag{6}$$

where

$$\begin{aligned} s_{\mathrm{HMW}} =& \frac{1}{\gamma_2-1}\left(\gamma_2 s_1 - s_2\right) - \frac{1}{\gamma_2+1}\left(\gamma_2 s_1 + s_2\right) \\ =& \frac{2\gamma_2}{\gamma_2^2-1}\left(s_1 - s_2\right) \end{aligned} \tag{7}$$

$$b_{\mathrm{HMW}} = \frac{1}{\gamma_2-1}\left(\gamma_2 b_1 - b_2\right) - \frac{1}{\gamma_2+1}\left(\gamma_2 d_1 + d_2\right) \tag{8}$$

In Eq. (6), $N_{\mathrm{WL}} = N_1 - N_2$ is the wide-lane ambiguity, $\lambda_{\mathrm{WL}} = \lambda_1\lambda_2/(\lambda_1 - \lambda_2)$ is the wide-lane wavelength. The HMW biases b_{HMW}, also more commonly known as wide-lane phase biases or wide-lane uncalibrated phase delays (WL UPDs), are estimated from the network processing and then distributed to users to help them achieve undifferenced ambiguity resolution (Ge et al. 2008; Geng et al. 2012). Similar to the case on DCBs, s_{HMW} can also be assimilated into b_{HMW} in the satellite wide-lane phase bias estimation. The specific form of s_{HMW} is given in (7), which is proportional to s_{GF} and scaled by a factor $2\gamma_2/(\gamma_2^2-1)$. This scaling factor is 3.967 for the GPS L1/L2 combination and about 3.537 for the Galileo E1/E5a combination.

Approximating the APC effect

The code/phase biases in least squares estimation can only absorb the part of the APC effect that is similar in nature to them. Since signal biases are assumed to originate from the GNSS hardware and remain relatively stable over short periods of time (Håkansson et al. 2017), they are typically parameterized as constant values within a processing period. However, the APC effect is highly variable with the signal direction (Schmid et al. 2007; Geng et al. 2021a). Fortunately, it has been shown in the clock analysis that the constant z-PCO can be a good approximation to the variable true satellite APC effect (Zhu et al. 2003; Cardellach et al. 2007). Here, we will quantify the maximum absolute errors that deviate from the constant approximations. As the APC effects of satellite antennas and receiver antennas behave differently, we decompose the combined APC effect here as

$$s_i = s_i^{\mathrm{sat}} + s_i^{\mathrm{rec}} \tag{9}$$

where s_i^{sat} is the satellite APC effect and s_i^{rec} is the receiver APC effect.

Satellite APC effect

The satellite APC model is defined in a body-fixed reference frame on the satellite. In the absolute APC model provided by the IGS ANTEX convention (Montenbruck et al. 2015), the satellite APC correction is given by the sum of a constant PCO vector and the orientation-specific PCVs with respect to the center of mass. The constant PCO vector can be expressed as $\mathbf{p}_i^{\text{sat}} = \left(x_i^{\text{sat}}, y_i^{\text{sat}}, z_i^{\text{sat}}\right)$ where the z-axis is along the radial direction. The PCVs are given as a grid $h_i^{\text{sat}}\left(\alpha^{\text{sat}}, \eta^{\text{sat}}\right)$ that depends on azimuth α^{sat} and nadir η^{sat}. The impact of satellite antenna PCO/PCVs is formulated as

$$s_i^{\text{sat}} = \mathbf{p}_i^{\text{sat}} \cdot \mathbf{e} + h_i^{\text{sat}}\left(\alpha^{\text{sat}}, \eta^{\text{sat}}\right) \tag{10}$$

where $\mathbf{e}$ is the unit vector in the line-of-sight (LOS) direction. The PCO vector $\mathbf{p}_i^{\text{sat}}$ is projected onto the LOS direction $\mathbf{e}$ through a dot product. This projection can be expanded as

$$\mathbf{p}_i^{\text{sat}} \cdot \mathbf{e} = x_i^{\text{sat}} \cos\alpha^{\text{sat}} \sin\eta^{\text{sat}} + y_i^{\text{sat}} \sin\alpha^{\text{sat}} \sin\eta^{\text{sat}} + z_i^{\text{sat}} \cos\eta^{\text{sat}} \tag{11}$$

It is important to note that the nadir angle η^{sat} between the LOS direction and the radial direction of the satellite is constrained by the geometric relationship between the earth and the satellite orbit. The nadir angle η^{sat} is less than 13.9° for GPS satellites and 12.5° for Galileo satellites (Geng et al. 2021a). This constraint implies that $z_i^{\text{sat}} \cos\eta^{\text{sat}}$ contributes the most to the PCO effect among the three components. Moreover, it is feasible to consider $z_i^{\text{sat}} \cos\eta^{\text{sat}}$ as a constant z_i^{sat} because the coefficient $\cos\eta^{\text{sat}}$ varies only between 0.97 and 1.00. Therefore, we assume that z-PCO z_i^{sat} is an approximation of the true APC effect s_i^{sat} and treat the other components as residuals from this approximation, which include the difference between the constant z-PCO and the projection of PCO vector, as well as the PCVs. The inter-frequency difference of satellite APC effect in (4) and (7) can be approximated as

$$s_1^{\text{sat}} - s_2^{\text{sat}} \approx z_1^{\text{sat}} - z_2^{\text{sat}} \tag{12}$$

To evaluate the effectiveness of such an approximation, we calculate the constant approximations $z_1^{\text{sat}} - z_2^{\text{sat}}$ and possible errors for antennas of all Galileo and GPS Block III satellites listed in the pilot IGS Repro3 ANTEX file i*gsR3_2135.atx* in 2020, and the result is depicted in Fig. 1. The possible errors are calculated by subtracting $z_1^{\text{sat}} - z_2^{\text{sat}}$ from the true APC effect $s_1^{\text{sat}} - s_2^{\text{sat}}$ within the limitation of nadir angles mentioned above. The colored numbers in the figure indicate the maximum absolute values of the approximation (bottom) and the maximum absolute errors (top) for the satellite antennas grouped by their blocks. The frequency combinations used for this calculation are L1/L2 for GPS and E1/E5a for Galileo, and they are the same for the rest of this article.

Although the inter-frequency difference of z-PCOs varies considerably among satellite antennas, the maximum absolute errors in the approximation are all in the range of 5 to 15 mm. For the antennas of Galileo In-Orbit Validation (IOV) satellites, the inter-frequency differences of z-PCOs are quite small, and all are below 100 mm. However, the errors in approximation of Galileo IOV antennas can vary by up to ± 10 mm, mainly due to the inter-frequency difference of the PCVs. The constant approximation performs best for Galileo Full Operational Capability (FOC) satellites antennas, with a maximum absolute error of less than 5.4 mm, whereas the inter-frequency difference of z-PCOs ranges from 40 to 180 mm. The antennas of GPS Block III satellites have the largest inter-frequency difference of z-PCOs and maximum absolute errors, at 491.9 mm and 15.1 mm, respectively. All GPS Block III satellite antennas

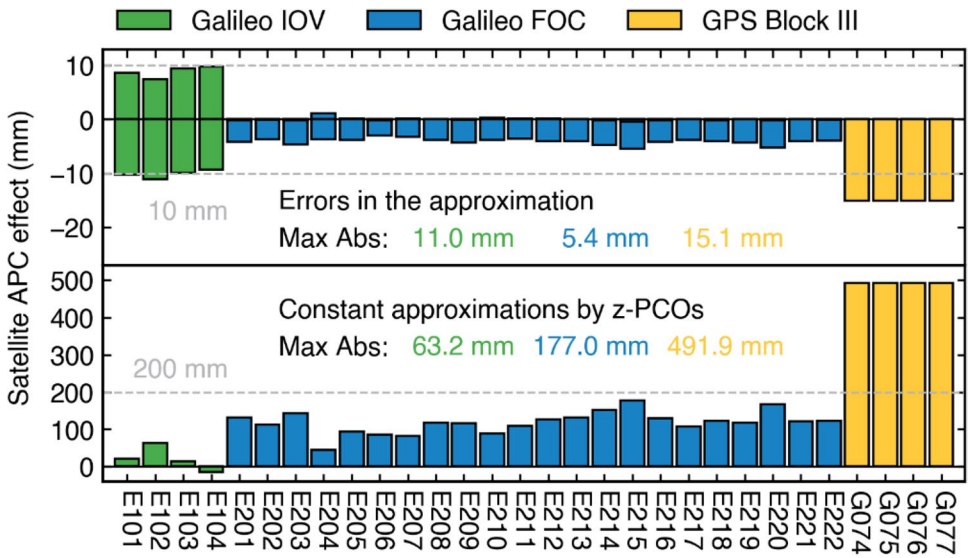

Fig. 1 Constant approximations and errors in the approximation of the inter-frequency difference of APC effects for antennas of Galileo and GPS Block III satellites listed in *igsR3_2135.atx*

share the same value as they all share the APC calibrations of G074. For most of these satellite antennas, but with the exception of Galileo IOV, the error in approximation comes mainly from the variation in $z_i^{\mathrm{sat}} \cos \eta^{\mathrm{sat}}$; thus, it is roughly proportional to the constant approximation $z_1^{\mathrm{sat}} - z_2^{\mathrm{sat}}$.

According to (3) and, an APC effect of 100 mm can introduce an offset of about 0.33 ns in DCB estimation and 0.45 cycles in wide-lane phase bias estimation for both L1/L2 and E1/E5a combination. For the data given in Fig. 1, the constant effect $z_1^{\mathrm{sat}} - z_2^{\mathrm{sat}}$ leads to a maximum change of 1.64 ns or 2.23 cycles for L1/L2 combination and 0.59 ns or 0.80 cycles for E1/E5a combination. This effect can seriously impact the wide-lane ambiguity resolution if the APC correction is not handled consistently between the analysis center and PPP-AR users. Also, the error in the approximation does not exceed 0.05 ns and 0.07 cycles for both L1/L2 and E1/E5a combinations, which is comparable to the observation noises and other uncorrected errors. Since these orientation-specific variations cannot be well absorbed into the bias estimates, they can be ignored without further concerns.

Receiver APC effect

Like the APC model for satellites, the APC of the receiver antenna can also be represented by a constant PCO vector $\mathbf{p}_i^{\mathrm{rec}} = \left(x_i^{\mathrm{rec}}, y_i^{\mathrm{rec}}, z_i^{\mathrm{rec}}\right)$ and a PCV grid $h_i^{\mathrm{rec}}(\alpha^{\mathrm{rec}}, \beta^{\mathrm{rec}})$, and the impact of receiver APCs is formulated as

$$s_i^{\mathrm{rec}} = \mathbf{p}_i^{\mathrm{rec}} \cdot \mathbf{e} + h_i^{\mathrm{rec}}(\alpha^{\mathrm{rec}}, \beta^{\mathrm{rec}}) \tag{13}$$

The difference is that the receiver APC model is described in a local reference frame with respect to the antenna reference point, where the angle between the LOS direction and the z-axis along the vertical direction is defined as zenith angle β^{rec}. For ground receiver antennas, the zenith angle of the LOS direction can vary from 0° to 90°, which allows s_i^{rec} to vary over a considerable range relative to its satellite counterpart. Therefore, the APC effect of receiver antennas cannot be approximated by any constant and can hardly be absorbed into the receiver code/phase biases.

Since the APC effect of receiver antennas acts on the same observations as the APC effect of satellite antennas, it still causes an impact on the estimation of parameters even other than the receiver code/phase biases, such as the wide-lane ambiguity of the HMW linear combinations. This effect is perhaps the greatest disadvantage of our approximate corrections compared to the strict corrections, and we are obligated to assess the potential errors that it introduces. We hence calculate the variation range of the receiver APC effects for about 110 antenna types listed in *igsR3_2135.atx* and used in Repro3 in the same way as in Fig. 1, and the results are presented in Fig. 2. The main difference is that no constant approximation is applied here. Almost all of these APC effects are within ± 30 mm, which is roughly equivalent to 0.10 ns in DCB and 0.14 cycles in wide-lane UPD. The maximum absolute is 36.4 mm for GPS receiver antennas and 42.1 mm for Galileo receiver antennas, as shown in Fig. 2.

In general, even the largest receiver APC effect is still smaller than the satellite APC effect from the Galileo FOC and GPS Block III satellites. However, the variation range of the receiver APC effect may be larger than its satellite counterpart. Longer observation periods can mitigate the highly variable receiver APC effect by taking the average. However, we note that some receiver antennas listed in *igsR3_2135.atx* have a variation range of APC effect of ± 60 mm (e.g.,

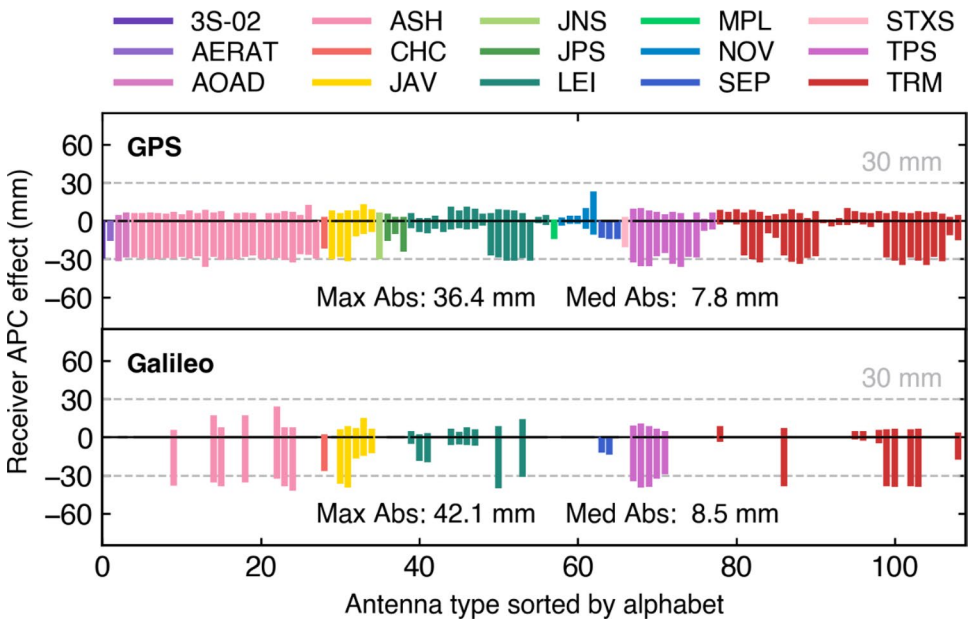

Fig. 2 Variation range of the inter-frequency difference of APC effects for receiver antennas employed in Repro3, APC calibrations come from *igsR3_2135.atx*. The acronyms on top of the figure are the first few letters common to the names of several antenna types

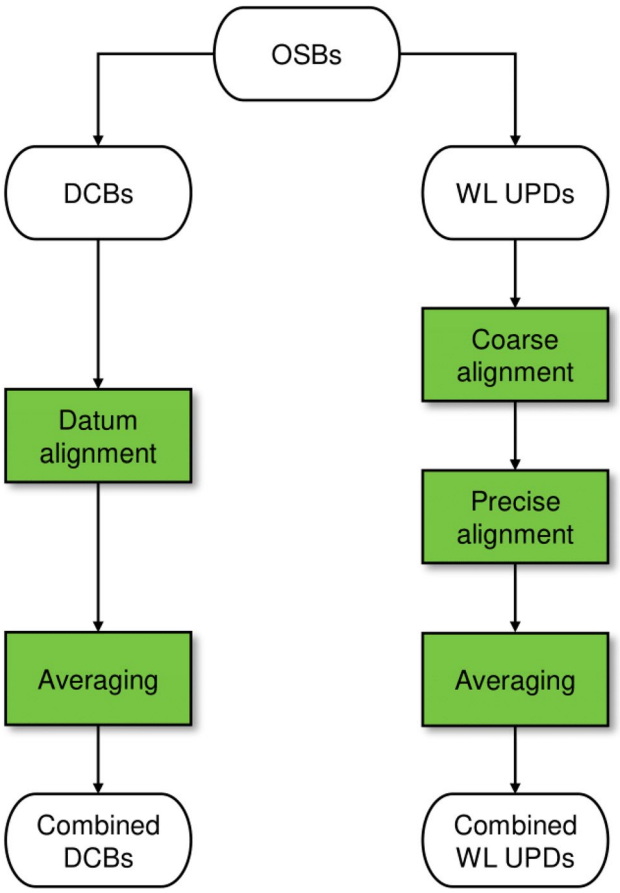

Fig. 3 Flowchart for the procedures to combine DCBs and wide-lane (WL) UPDs from code/phase biases provided by each AC

LEIAS05). Though these antennas are not used in Repro3, such an APC effect may still pose a threat to real-time PPP-AR applications with epoch-wise ambiguity resolution (Xin et al. 2020). Therefore, analysis centers and PPP-AR users must consider applying receiver APC corrections together with the satellite APC corrections to their geometry-free observations.

APC correction method

Following the conclusions of the previous section, we can correct the APC-affected satellite code/phase biases using only the z-PCO as a constant approximation and ignore the variation in the APC effect of up to about 1 cm. The code/phase biases we discuss here are the DCBs and wide-lane UPDs estimated from geometry-free observations. Since both the biases and the corrections mentioned in this section are for satellites, we ignore the superscript "sat" here for brevity. The APC-affected bias estimates are labeled with subscript "APC," and the symbol Δ is used to denote the approximate APC corrections. For the case of DCB, the correction equation is

$$\mathrm{DCB} = \mathrm{DCB}_{\mathrm{APC}} + \Delta\mathrm{DCB} \tag{14}$$

We know from (3) that the uncorrected APC effect on the GF observations s_{GF} will be absorbed by the DCB estimates. Replacing s_i in (4) with the approximation using z-PCOs, the correction for the affected DCBs should be

$$\Delta\mathrm{DCB} = -\left(z_1 - z_2\right) \tag{15}$$

This correction equation can be applied directly to the DCB products from the ionospheric analysis, such as the CODE's monthly DCB products. We particularly note that adding APC correction to DCB for a satellite will change the DCB datum associated with that value. For example, if the average of DCBs for all GPS satellites is set to zero, applying (14) to DCBs for any GPS Block III satellite will break this zero-mean condition (Montenbruck et al. 2014), and changes that occur in DCB datum will act on all DCBs from the same AC and for the same satellite constellation.

The correction equation for wide-lane UPDs can be formulated similarly, that is,

$$\mathrm{UPD}_{\mathrm{WL}} = \mathrm{UPD}_{\mathrm{WL,APC}} + \Delta\mathrm{UPD}_{\mathrm{WL}} \tag{16}$$

The wide-lane UPDs are expressed in cycles here. Taking account of (6) and (7), and then ignoring the change in the integer cycles of N_{WL}, the correction for the affected wide-lane UPDs can be obtained as

$$\lambda_{\mathrm{WL}}\Delta\mathrm{UPD}_{\mathrm{WL}} = -\frac{2\gamma_2}{\gamma_2^2 - 1}\left(z_1 - z_2\right) \tag{17}$$

which can be applied directly to products given in this form, such as GRG's integer clock products. Since most code/phase biases are now given in the observable-specific bias (OSB) representation defined in the Bias-SINEX format, it is inconvenient to apply APC corrections on the linear combinations of these biases. Fortunately, we can apply the linear transformation in Banville et al. (2020) to convert the APC correction in (15) and (17) to the observable-specific representation, where the corrections on the code OSB (Δd_i) and phase OSB (Δb_i) are

$$\Delta d_i = -\frac{\gamma_i^2}{\gamma_2^2 - 1}\Delta\mathrm{DCB} \tag{18}$$

$$\Delta b_i = +\frac{\gamma_i^2}{\gamma_2^2 - 1}\Delta\mathrm{DCB} - \frac{\gamma_i^2}{\gamma_2}\lambda_{\mathrm{WL}}\Delta\mathrm{UPD}_{\mathrm{WL}} \tag{19}$$

Equations (18) and (19) suggest that code OSBs d_i are affected only by ΔDCB while phase OSBs b_i are also affected

by $\Delta\mathrm{UPD}_{\mathrm{WL}}$. It should be noted that there are cases where the strict APC correction has been applied only to the HMW observations and not to the GF observations by the same AC and vice versa, examples of which are given in the next section. At this point, we will only apply (18) or (19) alone but not together. The APC corrections transformed into the observable-specific representation (Δd_i and Δb_i) are not consistent with the true APC effect s_i at that frequency, which implies that the affected OSBs cannot be used to resolve uncombined ambiguities. This is one of the reasons why the interoperability of bias products is compromised by the APC effect.

It is important to emphasize that the APC impact on DCBs and wide-lane UPDs is independent of each other. Applying APC correction to the DCBs does not affect the wide-lane UPDs and vice versa. Finally, we emphasize that the approximate APC corrections are independent of the bias estimates. They are constants and can be calculated directly from the PCO corrections in the IGS ANTEX file. But since the PCO corrections in the IGS ANTEX file are applied by adding to the observations rather than subtracting from them, it is $-z_i$ that the IGS ANTEX file provides.

Validation with clock/bias combination

The approximate APC correction methods are validated here with two bias combination exercises. The first combination is performed with the original IGS Repro3 clock/bias products for both GPS and Galileo satellites. The second combination is performed with the same clock products but with the approximate APC corrections applied to the bias products. These bias products are preprocessed differently because they are obtained by different processing strategies. The brief procedures for bias combination will be introduced later to facilitate the presentation of the experimental results.

Preprocessing

Table 1 shows the four ACs which provide code/phase bias products that implement PPP-AR for IGS Repro3 in the year 2020. All bias products have been transformed into OSBs for consistency. The approximate APC corrections in (18) and (19) are then directly applied to these OSBs. The specific corrections for $\Delta\mathrm{DCB}$ or $\Delta\mathrm{UPD}_{\mathrm{WL}}$ depend on the AC's processing strategy, and the differences among them are also summarized in Table 1; the ANTEX file *igsR3_2135.atx* is used to calculate the approximate APC corrections that are consistent with the IGS Repro3 convention

CODE and GRG employ a conventional processing strategy to estimate their phase biases where the APC correction for the HMW observations is not applied. The approximate APC correction for the wide-lane UPDs should thus be included in the preprocessing of these phase biases. Meanwhile, both CODE and GRG products are excluded from the DCB combination. CODE's daily DCBs for Repro3 are derived from the clock analysis (Villiger et al. 2019) and typically in a magnitude of about fractions of a nanosecond. They are in marked contrast to the DCBs derived from the ionospheric analysis and commonly in a magnitude of a few nanoseconds. GRG did not estimate code biases in their integer clock model. Therefore, for both CODE and GRG products, we assume $\Delta\mathrm{DCB} = 0$ and correct the phase OSBs with just (18).

The EMR product is transformed from the phase biases calculated by NRCan in conjunction with the monthly DCB products from the CODE's ionospheric analysis. In this case, NRCan has corrected the APC effect on the HMW observations, but such corrections have not been applied to the GF observations in the CODE's ionospheric analysis (Schaer 1999). We hence apply (18) and (19) to correct these biases and assume $\Delta\mathrm{UPD}_{\mathrm{WL}} = 0$.

TUG is the only AC that calculates its code/phase biases using the raw observation approach (Strasser et al. 2019; Strasser 2022). Since it is necessary to correct APC effects on the raw observations, no additional preprocessing is required for their products. The other ACs provide no code/phase bias products.

Combination procedures

The bias combination is implemented by PRIDE CKCOM, a clock/bias combination software package developed by Wuhan University. The procedure for the combination generally follows the approach Banville et al. (2020) proposed. The DCBs, wide-lane UPDs, and IF integer phase clocks are

Table 1 Overview of the analysis centers participating in the bias combination and the specific APC correction applied to their products

ID	Organization	Bias format	Approximate APC correction applied	
			DCB	WL UPD
COD	Center for Orbit Determination in Europe (CODE)	OSB	Inapplicable	Yes
EMR	Natural Resources Canada (NRCan)	OSB	Yes	No
GRG	Centre National d'Études Spatiales (CNES)	WL UPD	Inapplicable	Yes
TUG	Graz University of Technology	OSB	No	No

combined sequentially. This study focuses only on the APC effect on the combination of DCBs and wide-lane UPDs. These two combinations are practically independent of each other Fig. 3.

Before the combination, reconciling the bias datums set by ACs is important to ensure consistency among these products. A reference AC needs to be selected for the calculation of the datum differences between AC's products. Given that only products from EMR and TUG are involved in the DCB combination, we selected TUG as the reference AC, since TUG's DCBs are updated daily, while EMR's DCBs are updated monthly. The datum difference between each AC's DCBs and the reference AC's DCBs is calculated by taking the average difference between them. This datum difference is then removed from each AC's DCBs. After aligning the bias datum of each AC to that of the reference AC, the combined DCB estimates are directly the mean value of each AC's DCBs for each satellite. It also implies that each AC's DCBs are combined with equal weight.

The alignment of wide-lane UPDs is divided into two steps. The first step is the coarse alignment, where a reference satellite is selected, and then, the difference between an AC's wide-lane UPD and the reference AC's wide-lane UPD for this reference satellite is corrected from all satellite wide-lane UPDs provided by this AC. The second step is the precise alignment, where the common satellites to all ACs are picked out, and the mean values of each AC's wide-lane UPDs for the common satellites are then aligned to the reference AC's mean value. Similarly, the combined estimates are the mean value of each AC's wide-lane UPDs after two alignments.

It should be added that the datum alignments for the GPS and Galileo satellites are performed separately. Outliers in the combination are detected by comparing the median absolute deviation (MAD), which is the absolute value of the difference between the code/phase bias provided by an AC for a satellite and the median of these code/phase biases. After calculating the MAD for each AC, we take the average of these MADs and reject code/phase biases whose MAD exceeds the average by a factor of 4. The DCBs and wide-lane UPDs are given here as constant daily values.

Combination results

Figure 4 shows the mean residuals for each satellite from the DCB combination over the year 2020. Outliers and "zero residuals" (due to only one AC contributing the value for a satellite) have been removed to ensure that the residuals involved in the statistics result from a combination of two or more contributions. Since the only ACs involved in the DCB combination are EMR and TUG, their residuals are completely symmetrical. The DCB combination was not performed for Galileo satellites because EMR does not provide bias products for them.

When the approximate APC correction is not applied to the EMR's DCBs, the mean residuals of the GPS Block III satellites are about 0.72 ns, which is significantly larger than that of the other blocks of GPS satellites. This value is very close to half of the inter-frequency difference in the z-PCOs of their satellite antennas (equivalent to 0.82 ns). This is a good indication that the inter-frequency difference in z-PCOs is the major cause of the offset between the DCBs from TUG and EMR. However, there is also a difference of about 0.1 ns between the above-mentioned two numbers. This is because the approximate APC corrections result in the change of the DCB datum. Considering that the number of GPS satellites is 32, correcting APC effect for each GPS Block III satellite will contribute roughly 0.05 ns to the change in the DCB datum (i.e., 1/32 of its APC effect of about 1.64 ns). Thus, the four GPS Block III satellites in 2020 contributed a total of 0.2 ns to the change in the DCB datum, which is divided equally to the change in the mean residuals of the two ACs.

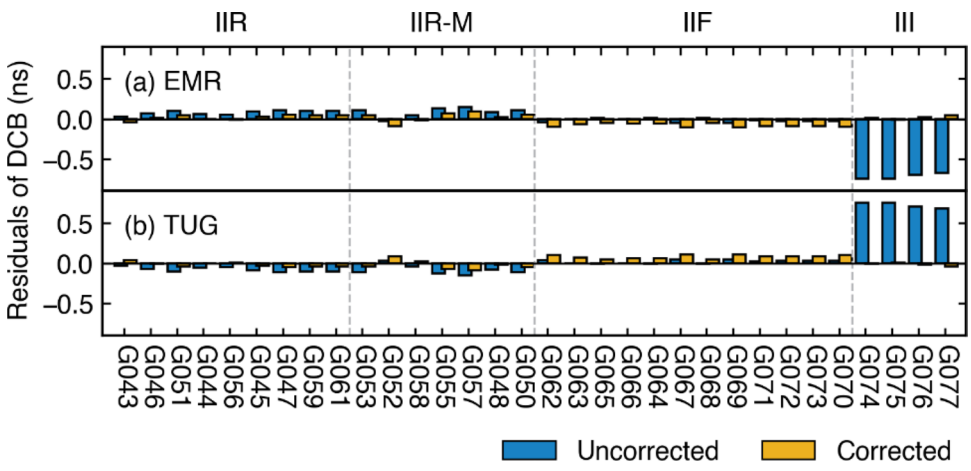

Fig. 4 Mean residuals from the DCB combination for each GPS satellite

After applying the approximate APC corrections to EMR's DCBs, the GPS Block III satellites show a 90% reduction in the mean residuals, confirming the effectiveness of our approximate APC corrections for DCBs. For other GPS satellites that are not affected by frequency-specific APC effects, such as GPS Block IIR and GPS Block IIF, the maximum absolute value of the mean residuals also decreased by nearly 30%. This can be attributed to the change in the DCB datum caused by the APC effect of GPS Block III satellites. However, we also note that for the GPS Block IIF satellites, the mean residuals increase by about 0.07 ns after applying the approximate APC corrections, which is a small but significant anomaly compared to the other satellites. We suspect that this may be related to the difference in the block-dependent correction models used by ACs in estimating the code biases or to the uncorrected APC effects. As the magnitude of this anomalous increase is less than 0.1 ns, comparable to the noise level of the DCB series, determining the exact cause of this abnormality is difficult and relies on a more careful examination of the products from each AC. Despite this, the mean residuals for all GPS satellites remained within 0.12 ns after applying the approximate APC correction.

Two residual series from the DCB combination are given in Fig. 5 as two typical examples. G074 is a GPS Block III satellite and G057 is a GPS IIR-M satellite. The residual series for G074 is missing for the first 25 days because EMR removed the satellite from its product on those days. The DCB residual series for both ACs were mutated between days 161 and 183. This is because on day 161 (June 10), G060 was taken out of service, bringing a change of about 0.28 ns in DCB datums. This datum change was immediately presented in the TUG's daily bias product, but was not updated to the monthly DCB used by the EMR until day 183 (July 1). Apart from these issues, the comparison of the residual series visually demonstrates the significantly increased consistency of the ACs' DCBs after applying the approximate APC corrections. We note that the approximate APC corrections are applied to EMR's DCBs but not to TUG's and that the corrected DCB series of G074 is shifted by about 1.5 ns in the positive direction relative to the uncorrected one.

The combinations of wide-lane UPDs for the GPS and Galileo satellites are performed separately. The mean residuals from the combination for each GPS satellite are plotted in Fig. 6. Note that TUG and NRCan applied APC corrections to the observations they used to estimate the phase biases while CODE and GRG did not. Like the performance in DCB combination, the maximum absolute value of mean residuals for all GPS satellites exceeds 0.15 cycles without correcting for APC effects but remains within 0.06 cycles after applying the approximate corrections. The mean residuals for some satellites have increased slightly after applying the approximate correction, which could be due to two different reasons. In the case where residuals have increased for all ACs, we suggest that this is similar to the cause of the anomaly in DCB combination, where the change in the datum of wide-lane UPDs has affected all wide-lane UPDs. Although most of these changes were in the direction of reducing residuals, errors in the product itself or in our approximate corrections may have caused an increase of a few tenths of a cycle in the wide-lane UPD residuals for some satellites; this topic is subject to further research. In the case that residuals increase for only a single AC, such as CODE's wide-lane UPD residuals provided for GPS Block IIR satellites, we believe that this is more likely related to the product's own issue. For these satellites, the combined estimates after applying approximate APC corrections are closer to the mean of the wide-lane UPDs of the other ACs but away from the wide-lane UPDs of CODE. While the

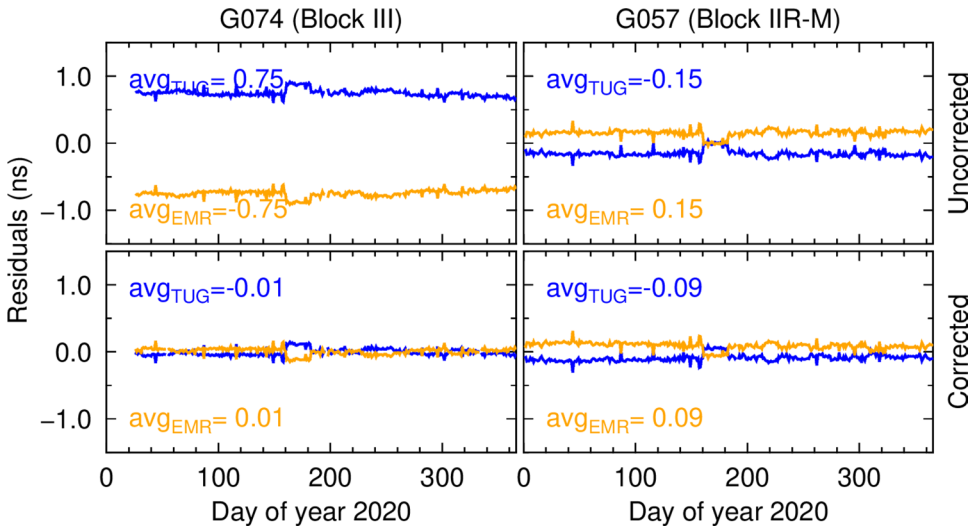

Fig. 5 Residual series from the DCB combination for G074 and G057

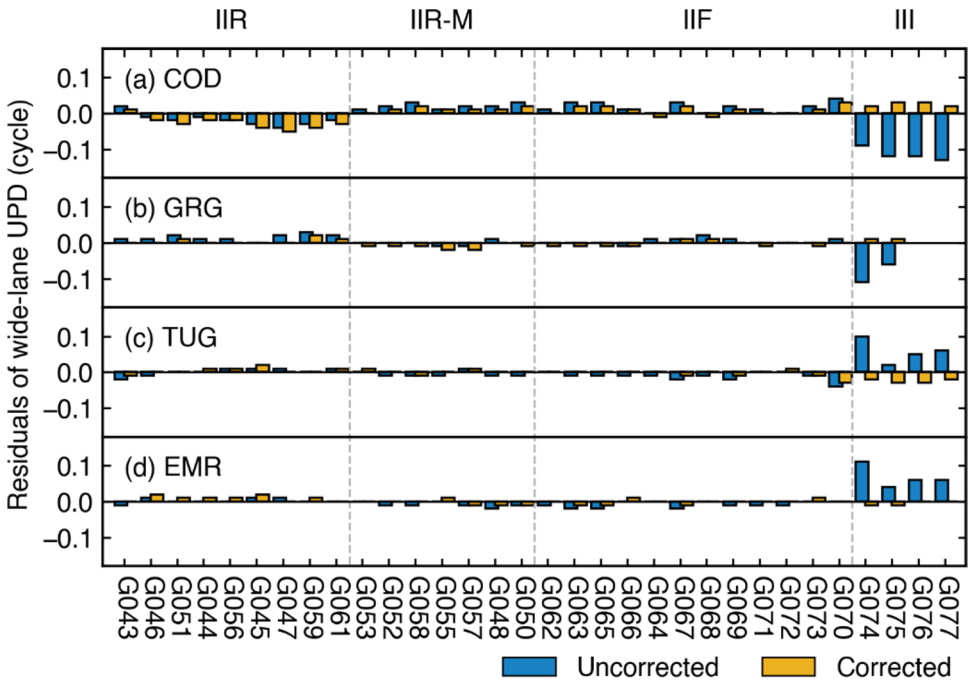

Fig. 6 Mean residuals from the wide-lane UPD combination for each GPS satellite

maximum mean residuals of CODE's wide-lane UPDs are within 0.06 cycles, the maximum mean residuals of the wide-lane UPDs from GRG, TUG, and EMR are guaranteed to be within 0.03 cycles. Overall, the approximate APC correction is very effective in terms of the goal of reducing the maximum residuals, despite interesting anomalies in the behavior of individual ACs or some satellites.

Unlike the case of GPS, wide-lane UPDs of all Galileo satellites are affected by their frequency-specific APC effects. The mean residuals for each Galileo satellite are plotted in Fig. 7. Some Galileo satellites show larger residuals from the combination of uncorrected wide-lane UPDs than the GPS Block III satellites, although the inter-frequency difference in z-PCOs for all Galileo satellites is less than half that of the GPS Block III satellites. The reason for the Galileo IOV satellites could be the larger differences in the ACs' processing strategies. But for the Galileo FOC satellites, this anomaly can be explained largely by the fact that only the fractional part of the APC effect will be absorbed into the wide-lane UPD, while the integer cycle part is indistinguishable from the integer ambiguity. In the combination of uncorrected products without EMR, the residuals of the TUG products are roughly the sum of the residuals of the other two ACs, with a maximum mean residual of 0.35 cycles. After applying the approximate APC correction, the mean residuals of all AC's wide-lane UPDs are within

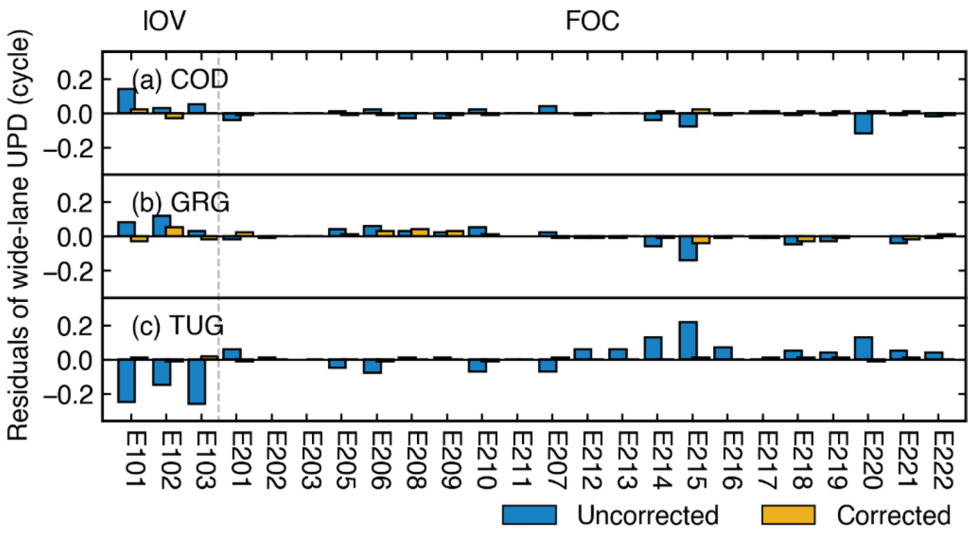

Fig. 7 Mean residuals from the wide-lane UPD combination for each Galileo satellite

0.06 cycles. Residuals for some Galileo satellites appear to be vacant, but, in fact, they are very small rather than zero. For example, in the combination for E203, while the approximate APC correction is not applied, the wide-lane UPDs from CODE and GRG are very consistent, and thus, TUG's contributions are identified as outliers and removed. After applying the approximate APC correction, the products of all three ACs were highly consistent and the residuals remained close to zero.

It is important to emphasize that correcting APC impact on maintaining consistency among the bias products is not only to reduce the residuals from the combination but also to ensure the stability of the combined estimates. We present residuals from the wide-lane UPD combination for two satellites in Fig. 8. For G074 on the top left, the residual series of CODE and GRG undergo sharp jumps of about 0.2 cycles in amplitude when data from the EMR or TUG are missing. After applying the approximate APC correction, the residual series are highly stable and consistent.

Such large jumps do not occur in series with complete data, such as the residual series for E102. Though the consistency among each AC's wide-lane UPDs improved after the correction, the oscillation levels of each residual series increased to about 0.05 cycles compared to the more stable case before the correction. As the wide-lane UPDs from CODE and TUG get closer, the GRG's wide-lane UPDs are more likely to be flagged as outliers and lead to more unstable combined estimates and combination residuals. A similar case is also found in the residual series for G074 in the upper left panel, where the EMR's wide-lane UPDs are missing in the first month of 2020, leaving consistent CODE's and GRG's contributions, and the TUG's wide-lane UPDs are thus removed by quality control. These anomalies suggest the need for more accurate detection of outliers in future studies. The apparently different behavior of GRG's wide-lane UPDs may be due to GRG's different processing strategies for Galileo IOV satellites. Despite the need for refinement in the strategies for removing outliers, the approximate APC correction is still beneficial in improving the consistency of the wide-lane UPDs and helps expose issues in AC's products.

Finally, we summarize the overall statistics of this combination practice for each type of satellite in Table 2. For the mean standard deviation (STD) of the combined estimates, the bias products whose stability is most affected by the uncorrected APC effect are those for the GPS Block III satellites, which are in the commissioning phase and suffer the most from data outages. The other GPS satellites are affected to a lesser extent. The Galileo satellites, with the least amount of missing data, show little degradation in stability. After the correction, the mean STDs of the combined DCB series for GPS Block III satellites reduce by more than 60%. Good stability of about 0.1 ns for the combined DCB series and below 0.1 cycles for the combined wide-lane UPD series can be achieved. The mean root mean square (RMS) residuals of individual bias products are ensured within 0.1 ns for DCBs and 0.03 cycles for wide-lane UPDs by the approximate APC corrections.

In conclusion, the stability of the combined estimates depends on the consistency of the bias products from different ACs, which are quite susceptible to the uncorrected APC effects. The combination results verify that the approximate APC corrections can effectively restore the interoperability between these bias products, thus ensuring the acquisition of high-quality combined bias products.

Validation with PPP-AR

We aim to verify the equivalent performance between the APC approximately corrected and the APC strictly corrected

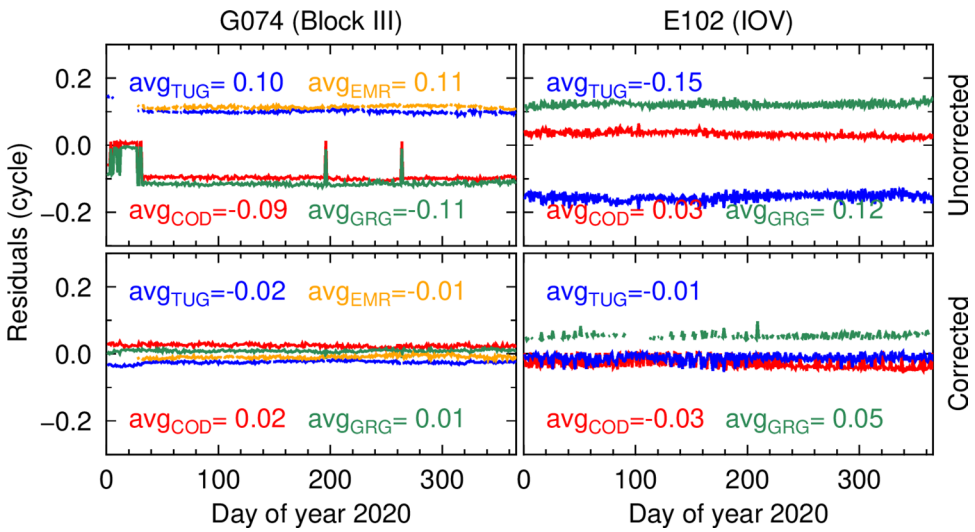

Fig. 8 Residual series from the wide-lane UPD combination of G074 and E102

Table 2 Mean STDs of the combined estimates and mean RMS residuals of individual bias products from each analysis center

	GPS (not Block III)		GPS Block III		Galileo	
	Uncorrected	Corrected	Uncorrected	Corrected	Uncorrected	Corrected
DCB combined estimates and residuals (in nanoseconds)						
CMB STD	0.14	0.13	0.25	0.09	\	\
EMR RMS	0.09	0.08	0.72	0.05	\	\
TUG RMS	0.09	0.08	0.72	0.05	\	\
Wide-lane UPD combined estimates and residuals (in cycles)						
CMB STD	0.03	0.03	0.04	0.02	0.09	0.09
COD RMS	0.02	0.02	0.12	0.03	0.03	0.01
GRG RMS	0.01	0.01	0.10	0.01	0.04	0.02
TUG RMS	0.01	0.01	0.07	0.03	0.08	0.01
EMR RMS	0.01	0.01	0.08	0.01	\	\

combined clock/bias products in PPP-AR. However, for IGS repro3, only two ACs (TUG and NRCan) provide bias products with rigorous APC correction in their processing strategies, and Galileo satellites are excluded from the NRCan's products. In order to obtain suitable products for this validation, we re-calculate two sets of clock/bias products using the processing strategy to generate routine products from the Wuhan University (WHU) with and without APC corrections on the HMW observations. The WHU products without APC correction are then corrected by the approximate APC corrections and combined with the TUG products to obtain APC approximately corrected combined bias products. The strictly corrected combined bias products are obtained from the TUG and the WHU products generated with rigorous APC corrections. Therefore, the APC approximately corrected combined products contain possible uncorrected satellite PCO/PCV effects and receiver PCO/PCV effects from the APC-affected WHU products, while the APC strictly corrected combined products do not. Only satellite clock/bias products are combined. The other products for PPP-AR, such as satellite ephemerides and attitudes, are complemented by TUG products.

Figure 9 shows the 183 IGS stations used to generate the WHU products and the 90 IGS stations used for PPP-AR processing. Daily GPS and Galileo data from these stations for the first 30 days of 2020 are processed with the combined clock/bias products mentioned above in the same configuration and static mode. The PPP-AR processing is done by PRIDE PPP-AR, an open-source software developed by Wuhan University (Geng et al. 2019a, 2021b).

The distribution of all single-differenced wide-lane ambiguity residuals from the PPP-AR processing is plotted in Fig. 10. Both the APC approximately corrected and APC strictly corrected combined products perform almost identically in terms of ambiguity resolution, with STDs of the ambiguity residuals around 0.10 cycles for both GPS and Galileo satellites. However, it is unexpected that the approximate APC correction results in about 1% more wide-lane

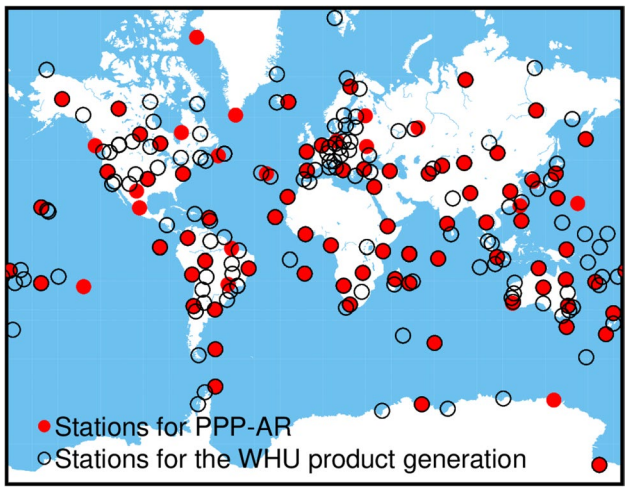

Fig. 9 Distribution of the stations for PPP-AR and the WHU product generation

ambiguity residuals falling within ±0.1 cycles compared to the rigorous APC correction. We speculate that this subtle difference may arise from the difference in the models used to generate the clock/bias products and cannot be used as significant evidence to determine superiority since only two contributions are combined.

The estimated coordinates from the PPP-AR processing are compared against the weekly IGS1R03 SINEX solutions, and a daily 7-parameter Helmert transformation is performed to align the reference frame. The resulting mean RMS residuals in each direction are listed in Table 3. In general, the approximate APC correction and rigorous APC correction can be considered to have the same effect on the positioning. The wide-lane ambiguity fixing rates with a round-off criterion of 0.2 cycles are also presented in Table 3, where a small difference of only 0.2% is found between the two combined products.

In summary, compared to the mean wide-lane ambiguity fixing rate of over 90% and the positioning accuracy of

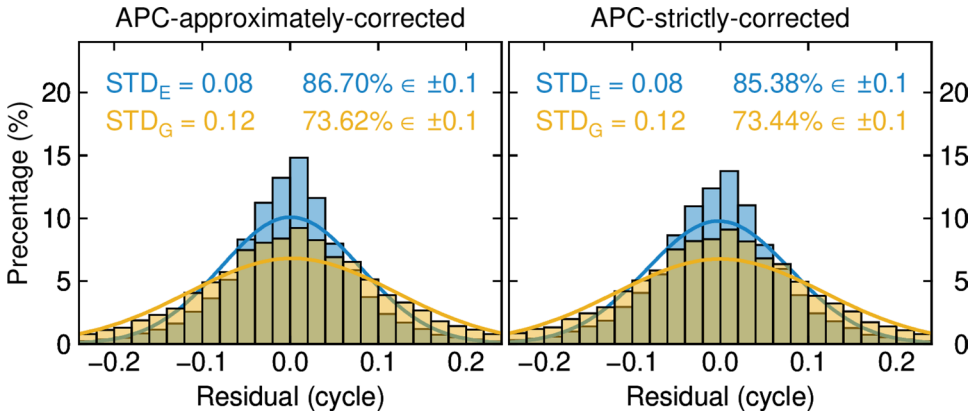

Fig. 10 Distribution of all single-differenced wide-lane ambiguity residuals from the PPP-AR processing with APC approximately corrected and APC strictly corrected combined bias products

Table 3 Mean positioning RMS (mm) residuals and wide-lane ambiguity fixing rates

Products type	Positioning RMS (mm)			Fixing rate (%)	
	East	North	Up	GPS	Galileo
APC approximately corrected	1.35	1.42	6.31	91.80	97.53
APC strictly corrected	1.34	1.43	6.33	91.57	97.30

several millimeters, we believe that there is no difference in the PPP-AR performance of the APC approximately corrected and APC strictly corrected combined products. Although the approximate APC correction seems to have a small advantage in the wide-lane ambiguity resolution in this PPP-AR processing, we attribute this unexpected result to the insufficient contributions to the combination. Further studies and more contributions are still needed to clarify the subtle differences between these two correction methods.

Conclusions and outlook

This study analyzed the frequency-specific APC impacts on the code/bias estimation. The bias products generated without applying APC corrections on observations (e.g., CODE and GRG) will lose their interoperability with the bias products generated with APC corrections on observations applied (e.g., TUG). Such effects can exceed 1.6 ns on GF observations or DCBs and 2.2 cycles on HMW observations or wide-lane phase biases for the current GPS Block III and Galileo satellites.

The loss of interoperability can be fatal for the IGS Repro3 bias combination. The consistency between the bias products from different ACs is destroyed by the uncorrected APC effects, and therefore, the availability and stability of the combined bias products cannot be guaranteed. To reconcile these bias products for IGS Repro3, we propose an approximate APC correction method that uses constant satellite z-PCOs instead of the varying true APC effects. With this approximate APC correction, interoperability between the IGS repro3 bias products can be effectively restored, and the mean RMS residuals are controlled to within 0.1 ns in the DCB combination and within 0.03 cycles in the wide-lane UPD combination.

PPP-AR processing using the experimental products combined from the WHU and TUG products shows that there is only a small difference of 0.2% in the wide-lane ambiguity fixing rate between the APC approximately corrected and APC strictly corrected combined bias products. This means that the PPP-AR users can apply approximate APC corrections to convert bias products from any analysis center without further concern. For example, remove the absorbed APC effect from the bias product in order to apply it to resolve uncombined ambiguities.

At the 2022 IGS Virtual Workshop, an agreement on correcting the APC effects in the processing strategy was reached by the ACs (Geng 2022), which is expected to facilitate the interoperability of the generated bias products. In IGSMAIL-8279 released on November 21, 2022, by the IGS PPP-AR Working Group, it has been announced that each AC needs to apply APC corrections on their geometry-free bias generations, and a new keyword "APC_MODEL" in the Bias-SINEX is introduced to designate this APC model. However, the approximate APC corrections still take advantage of simplicity and not requiring adjustments of orbits and clocks. This convenience is particularly beneficial for reconciling the numerous bias products during the IGS Repro3 period. Due to the practical situation of the current PPP-AR bias products, the APC effects on multi-frequency bias products and BDS bias products have not been discussed. We believe that correcting APC effects can restore the natural physical properties of the code/phase biases, which may be important for the all-frequency and all-GNSS applications and is expected to be further studied.

Acknowledgements We thank Sebastian Strasser for providing reference satellite attitudes and the IGS analysis centers for providing

Repro3 satellite products. The work for generating WHU clock/bias products and PPP-AR processing was facilitated by the supercomputing system at Wuhan University. This work is coordinated within the IGS PPP-AR Working Group. The National Science Foundation of China (42025401) and Hubei Luojia Laboratory (220100021) funded this study.

Author contributions JG developed the initial concepts and designed the research. JL detailed the concepts and drafted the paper. JL, ZY, and QZ performed the experiment. JG and SM revised the paper. All authors approved the manuscript.

Data availability The IGS repro3 products and GNSS observations used in this study can be accessed publicly at https://cddis.nasa.gov/archive/gnss/products/repro3/ and https://cddis.nasa.gov/archive/gps/data/daily/. The Repro3 combination products with approximate APC corrections applied are labeled as "IGS2R03FIN" therein (see IGS-MAIL-8248). The open-source PRIDE PPP-AR v2.2 software package can be downloaded at https://github.com/PrideLab/PRIDE-PPPAR/.

Declarations

Competing interests The authors declare no competing interests.

References

Banville S, Geng J, Loyer S, Schaer S, Springer T, Strasser S (2020) On the interoperability of IGS products for precise point positioning with ambiguity resolution. J Geod 94(1):1–15. https://doi.org/10.1007/s00190-019-01335-w

Cardellach E, Elósegui P, Davis JL (2007) Global distortion of GPS networks associated with satellite antenna model errors. J Geophys Res Solid Earth 112(7):1–13. https://doi.org/10.1029/2006JB004675

Collins P, Bisnath S, Lahaye F, Héroux P (2010) Undifferenced GPS ambiguity resolution using the decoupled clock model and ambiguity datum fixing. Navigation 57(2):123–135. https://doi.org/10.1002/j.2161-4296.2010.tb01772.x

Dach R, Selmke I, Villiger A, Arnold D, Prange L, Schaer S, Sidorov D, Stebler P, Jäggi A, Hugentobler U (2021) Review of recent GNSS modelling improvements based on CODEs Repro3 contribution. Adv Sp Res 68(3):1263–1280. https://doi.org/10.1016/j.asr.2021.04.046

Dilssner F (2010) GPS IIF-1 Satellite Antenna Phase Center and Attitude Modeling. Inside GNSS 5(6):59–64

Dilssner F, Springer T, Enderle W, Office NS (2016) Evaluating the pre-flight GPS Block IIR/IIR-M antenna phase pattern measurements. In: IGS Workshop 2016. Sydney, Australia, 8–12 Feb

European GNSS Agency (2017) Galileo Satellite Metadata. https://www.gsc-europa.eu/support-to-developers/galileo-satellite-metadata.

Ge M, Gendt G, Rothacher M, Shi C, Liu J (2008) Resolution of GPS carrier-phase ambiguities in Precise Point Positioning (PPP) with daily observations. J Geod 82(7):389–399. https://doi.org/10.1007/s00190-007-0187-4

Geng J, Teferle FN, Shi C, Meng X, Dodson AH, Liu J (2009) Ambiguity resolution in precise point positioning with hourly data. GPS Solut 13(4):263–270. https://doi.org/10.1007/s10291-009-0119-2

Geng J, Shi C, Ge M, Dodson AH, Lou Y, Zhao Q, Liu J (2012) Improving the estimation of fractional-cycle biases for ambiguity resolution in precise point positioning. J Geod 86(8):579–589. https://doi.org/10.1007/s00190-011-0537-0

Geng J, Chen X, Pan Y, Mao S, Li C, Zhou J, Zhang K (2019a) PRIDE PPP-AR: an open-source software for GPS PPP ambiguity resolution. GPS Solut 23(4):1–10. https://doi.org/10.1007/s10291-019-0888-1

Geng J, Chen X, Pan Y, Zhao Q (2019b) A modified phase clock/bias model to improve PPP ambiguity resolution at Wuhan University. J Geod 93(10):2053–2067. https://doi.org/10.1007/s00190-019-01301-6

Geng J, Guo J, Wang C, Zhang Q (2021a) Satellite antenna phase center errors: magnified threat to multi-frequency PPP ambiguity resolution. J Geod 95(6):1–18. https://doi.org/10.1007/s00190-021-01526-4

Geng J, Yang S, Guo J (2021b) Assessing IGS GPS/Galileo/BDS-2/BDS-3 phase bias products with PRIDE PPP-AR. Satell Navig. https://doi.org/10.1186/s43020-021-00049-9

Geng J (2022) Recommendations for Precise Point Positioning with Ambiguity Resolution (PPP-AR). In: IGS 2022 Virtual Workshop, 27 June–1 July

Håkansson M, Jensen ABO, Horemuz M, Hedling G (2017) Review of code and phase biases in multi-GNSS positioning. GPS Solut 21(3):849–860. https://doi.org/10.1007/s10291-016-0572-7

Hatch R (1982) The synergism of GPS code and carrier measurements. In: Proceedings of the Third International Symposium on Satellite Doppler Positioning at Physical Sciences Laboratory of New Mexico State University. Feb. 8–12, Vol. 2, pp 1213–1231

Johnston G, Riddell A, Hausler G (2017) The International GNSS Service. In: Teunissen PJG, Montenbruck O (eds) Springer Handbook of Global Navigation Satellite Systems. Springer, Cham, Switzerland, pp 967–982

Katsigianni G, Loyer S, Perosanz F, Mercier F, Zajdel R, Sośnica K (2019) Improving Galileo orbit determination using zero-difference ambiguity fixing in a Multi-GNSS processing. Adv Sp Res 63(9):2952–2963. https://doi.org/10.1016/j.asr.2018.08.035

Laurichesse D, Mercier F, Berthias JP, Broca P, Cerri L (2009) Integer ambiguity resolution on undifferenced GPS phase measurements and its application to PPP and satellite precise orbit determination. Navigation 56(2):135–149. https://doi.org/10.1002/j.2161-4296.2009.tb01750.x

Laurichesse D (2011) The CNES Real-time PPP with undifferenced integer ambiguity resolution demonstrator. In: Proceedings of ION GNSS 2011, Institute of Navigation, Portland, Oregon, USA, pp 654–662

Loyer S, Perosanz F, Mercier F, Capdeville H, Marty JC (2012) Zero-difference GPS ambiguity resolution at CNES-CLS IGS Analysis Center. J Geod 86(11):991–1003. https://doi.org/10.1007/s00190-012-0559-2

Melbourne WG (1985) The case for ranging in GPS-based geodetic systems. In: Proceedings of the first international symposium on precise positioning with the Global Positioning System. Rockville, Maryland, USA, pp 373–386

Montenbruck O, Hauschild A, Steigenberger P (2014) Differential Code Bias Estimation using Multi-GNSS Observations and Global Ionosphere Maps. Navigation 61(3):191–201. https://doi.org/10.1002/navi.64

Montenbruck O, Schmid R, Mercier F, Steigenberger P, Noll C, Fatkulin R, Kogure S, Ganeshan AS (2015) GNSS satellite geometry and attitude models. Adv Sp Res 56(6):1015–1029. https://doi.org/10.1016/j.asr.2015.06.019

Rothacher M, Schmid R (2010) ANTEX: the antenna exchange format version 1.4 International GNSS Service. Pasadena California, USA

Schaer S, Villiger A, Arnold D, Dach R, Prange L, Jäggi A (2021) The CODE ambiguity-fixed clock and phase bias analysis products: generation properties and performance. J Geod 95(7):1–25. https://doi.org/10.1007/s00190-021-01521-9

Schaer S (1999) Mapping and predicting the earth's ionosphere using the Global Positioning System. Ph.D. Thesis, University of Bern, Bern, Switzerland

Schaer S (2016) SINEX_BIAS—Solution (Software/technique) INdependent EXchange Format for GNSS BIASes Version 1.00. In: IGS Workshop on GNSS biases, Bern, Switzerland, November 5–6, 2015

Schmid R, Rothacher M (2003) Estimation of elevation-dependent satellite antenna phase center variations of GPS satellites. J Geod 77(7–8):440–446. https://doi.org/10.1007/s00190-003-0339-0

Schmid R, Steigenberger P, Gendt G, Ge M, Rothacher M (2007) Generation of a consistent absolute phase-center correction model for GPS receiver and satellite antennas. J Geod 81(12):781–798. https://doi.org/10.1007/s00190-007-0148-y

Steigenberger P, Thoelert S, Montenbruck O (2020) GPS III Vespucci: results of half a year in orbit. Adv Space Res. https://doi.org/10.1016/j.asr.2020.03.026

Strasser S, Mayer-Gürr T, Zehentner N (2019) Processing of GNSS constellations and ground station networks using the raw observation approach. J Geod 93(7):1045–1057. https://doi.org/10.1007/s00190-018-1223-2

Strasser S (2022) Reprocessing Multiple GNSS Constellations and a Global Station Network from 1994 to 2020 with the Raw Observation Approach. Ph.D. Thesis Graz University of Technology, Graz, Austria

Villiger A, Dach R (2021) International GNSS Service Technical Report 2020 (IGS Annual Report). Bern, Switzerland

Villiger A, Schaer S, Dach R, Prange L, Sušnik A, Jäggi A (2019) Determination of GNSS pseudo-absolute code biases and their long-term combination. J Geod 93(9):1487–1500. https://doi.org/10.1007/s00190-019-01262-w

Wanninger L, Sumaya H, Beer S (2017) Group delay variations of GPS transmitting and receiving antennas. J Geod 91(9):1099–1116. https://doi.org/10.1007/s00190-017-1012-3

Wübbena G (1985) Software developments for geodetic positioning with GPS using TI-4100 code and carrier measurements. In: Proceedings of the first international symposium on precise positioning with the Global Positioning System. Rockville, Maryland, USA, pp 403–412

Xin S, Geng J, Guo J, Meng X (2020) On the choice of the third-frequency Galileo signals in accelerating PPP ambiguity resolution in case of receiver antenna phase center errors. Remote Sens 12(8):1315. https://doi.org/10.3390/RS12081315

Zhu SY, Massmann FH, Yu Y, Reigber C (2003) Satellite antenna phase center offsets and scale errors in GPS solutions. J Geod 76(11–12):668–672. https://doi.org/10.1007/s00190-002-0294-1

Jihang Lin is currently a master's candidate at GNSS Research Center, Wuhan University. He received his bachelor's degree in geomatics engineering at the School of Geodesy and Geomatics, Wuhan University, in 2021. His main research now focuses on high-precision GNSS and its applications.

Jianghui Geng has been a professor in GNSS geodesy at Wuhan University since 2015. He graduated from the University of Nottingham in the UK in 2011. Afterward, he had an enterprise fellowship from the Nottingham Geospatial Institute in 2011 and a Green scholarship from the Scripps Institution of Oceanography from 2012 to 2014. His major research interest is high-precision GNSS.

Zhe Yan is a master's candidate at GNSS Research Center, Wuhan University. He received his bachelor's degree in geomatics engineering at the School of Geodesy and Geomatics, Wuhan University, in 2022. His main activity now is to combine clock/bias products for the third reprocessing effort.

Salim Masoumi obtained a Ph.D. in 2017 from the Australian National University, Research School of Earth Sciences. Since then, he has been working in the field of GNSS Analysis Section at Geoscience Australia. He has been coordinating the activities of the IGS analysis centers for the third reprocessing effort.

Qiyuan Zhang received his bachelor's degree in geomatics engineering at the School of Geodesy and Geomatics, Wuhan University, in 2018, and is a Ph.D. candidate at the GNSS Research Center, Wuhan University. His main activity is analyzing and generating phase clock/bias products.